REPORT DOCUMENTATION PAGE

1a. REPORT SECURITY CLASSIFICATION: Unclassified	1b. RESTRICTIVE MARKINGS
2a. SECURITY CLASSIFICATION AUTHORITY	3. DISTRIBUTION/AVAILABILITY OF REPORT: Approved for public release; distribution unlimited.
AD-A202 254	5. MONITORING ORGANIZATION REPORT NUMBER(S): ARO 23087.12-EL
6a. NAME OF PERFORMING ORGANIZATION: University of Pennsylvania	6b. OFFICE SYMBOL (If applicable)
7a. NAME OF MONITORING ORGANIZATION: U. S. Army Research Office	
6c. ADDRESS (City, State, and ZIP Code): Dept. of Electrical Engineering, Philadelphia, Pa 19104	7b. ADDRESS (City, State, and ZIP Code): P. O. Box 12211, Research Triangle Park, NC 27709-2211
8a. NAME OF FUNDING/SPONSORING ORGANIZATION: U. S. Army Research Office	8b. OFFICE SYMBOL (If applicable)
9. PROCUREMENT INSTRUMENT IDENTIFICATION NUMBER: DAAG29-85-K-0247	
8c. ADDRESS (City, State, and ZIP Code): P. O. Box 12211, Research Triangle Park, NC 27709-2211	10. SOURCE OF FUNDING NUMBERS: PROGRAM ELEMENT NO. / PROJECT NO. / TASK NO. / WORK UNIT ACCESSION NO.

11. TITLE (Include Security Classification): Research in Data Compression for Microwave Imagery and Its Effect Upon Image Quality

12. PERSONAL AUTHOR(S): Zhongjie Liang, Bernard Steinbert, Stanislav Kesler

13a. TYPE OF REPORT	13b. TIME COVERED	14. DATE OF REPORT (Year, Month, Day)	15. PAGE COUNT
Final	FROM 10/1/85 TO 9/30/88	Nov 11, 1988	48

16. SUPPLEMENTARY NOTATION: The view, opinions and/or findings contained in this report are those of the author(s) and should not be construed as an official Department of the Army position, policy, or decision, unless so designated by other documentation.

17. COSATI CODES		
FIELD	GROUP	SUB-GROUP

18. SUBJECT TERMS (Continue on reverse if necessary and identify by block number): Data Compression, Microwave Imagery, Image Quality, Optical Quantizer Design,

19. ABSTRACT (Continue on reverse if necessary and identify by block number)

In microwave imaging, aperture data are digitized, while system performance is determined by the quality of the image, which is usually a Fourier Transform of the aperture data. This research develops a methodology for finding a quantizer in the aperture domain which optimizes an image plane quality criterion.

For amplitude-phase quantization of complex data, a novel optimality criterion is posed which leads to a new and simpler optimal quantizer design.

20. DISTRIBUTION/AVAILABILITY OF ABSTRACT	21. ABSTRACT SECURITY CLASSIFICATION
☐ UNCLASSIFIED/UNLIMITED ☐ SAME AS RPT. ☐ DTIC USERS	Unclassified
22a. NAME OF RESPONSIBLE INDIVIDUAL	22b. TELEPHONE (Include Area Code) / 22c. OFFICE SYMBOL

The effectiveness of the theory is evaluated with computer simulation and on experimental data. The theory explains why fewer bits are satisfactory in reconstructed image, and it provides an analytical basis and a rule of thumb for bit allocation between amplitude and phase.

The theory imposes substantially no constraints upon the distributions of amplitude and phase in the microwave data. It is also shown that the optimum quantization design derived from the theory is nearly scene-independent and may achieve real-time performance.

Finally, the theory provides useful guidelines to analyze the nature of distortion due to data compression.

UP-VFRC-15-88

November 11, 1988

RESEARCH IN DATA COMPRESSION FOR MICROWAVE IMAGERY AND ITS EFFECT UPON IMAGE QUALITY

Zhongjie Liang

Bernard Steinberg

Stanislav Kesler

FINAL REPORT

CONTRACT NO. DAAG29-85-K-0247

Valley Forge Research Center
University of Pennsylvania
The Moore School of Electrical Engineering
Philadelphia, Pennsylvania 19104

PREFACE

Research under the contract has been conducted to the subject of data compression for microwave imagery. A theory of Bit Compression has been developed for compressing the aperture data in a microwave antenna array. Two papers have been sent to IEEE for publication. The first paper: "Optimum Data Quantization in Microwave Imagery and Its Effect Upon Image Quality" is to be published in IEEE Transactions on Acoustics Speech Signal Processing of December 1988, and the second paper:"An Exact Solution of the Analytic Equation of Image Quality from Optimum Quantization of Microwave Imaging Data" is currently under review.

In this report, the objective of this research is reviewed, the major procedure of theoretical development is demonstrated and the important results are discussed.

The mathematical derivation will not be shown in every detail in the report and could be found in the papers.

TABLES OF CONTENTS

LIST OF TABLES

LIST OF ILLUSTRATIONS

ABSTRACT

In microwave imaging, aperture data are digitized, while system performance is determined by the quality of the image, which is usually a Fourier Transform of the aperture data. This research develops a methodology for finding a quantizer in the aperture domain which optimizes an image plane quality criterion.

For amplitude-phase quantization of complex data, a novel optimality criterion is posed which leads to a new and simpler optimal quantizer design.

The effectiveness of the theory is evaluated with computer simulation and on experimental data. The theory explains why fewer bits are satisfactory in reconstructed image, and it provides an analytical basis and a rule of thumb for bit allocation between amplitude and phase.

The theory imposes substantially no constraints upon the distributions of amplitude and phase in the microwave data. It is also shown that the optimum quantization design derived from the theory is nearly scene-independent and may achieve real-time performance.

Finally, the theory provides useful guidelines to analyze the nature of distortion due to data compression.

1. INTRODUCTION

A high resolution microwave imaging system must process huge amounts of data. Because of the limitations on processing time, memory space and the cost of processor hardware, it is important to develop techniques to reduce the data handling requirement.

The data handling rate denoted by R is the product of the number of the samples denoted by N (which is the number of antenna array elements), the bandwidth of the signal denoted by B and the bit per sample denoted by b (bit is used as the information carrying unit). Namely,

$$R = NBb \text{ (bit/second)}$$

High cross-range resolution requires large number of elements and high range resolution requires large bandwidth. Therefore, for high resolution imaging system, the problem of reducing data handling requirement is addressed to bit compression which is the minimization of the number of bits per sample used to represent the image.

Techniques of this sort are usually referred to a more general term as data compression[1]. Unfortunately, most existing data compression techniques are found not to be useful for our application in microwave imaging because

1) In applying these techniques, both the input and the output of the compression processor are in the same domain. For microwave imaging, the data need to be compressed are the aperture data which are the complex samples of the electric field taken by the receiving antenna, which is usually a phased array [2]. The image is related to the aperture data by a diffraction integral of physical optics [3], which is well approximated by a Fourier transform when the distance from source to antenna is large enough [4]. In other words, the expected input and output of a compression processor are in different domains related by an integral transformation. It is the nature of integral transformation that any point in the transform domain does not correspond to a point in the source domain, but to the entire

source; As a result, the image quality criteria which govern the data compression algorithms are no longer valid.

2) The performance of data compression technique is measured by the capability of compression (e.g. compression ratio which is the ratio of the number of bits per pixel used for coding the data-compressed image to the number of bits per pixel used for coding the original image). However, from image fidelity point of view, the higher the compression is, the larger the distortion is. Therefore, in order to turn these techniques into a useful application in image processing, one requires not an arbitrary high compression scheme but the best trade off between the image fidelity and the degree of compression for given system constraint. In other words, one needs to know how the image quality is related to the controlled parameters of the compression processor, so that for given image quality requirement, one can determine what minimum number of bits that the data can be compressed to or, for given number of bits limited by the system, what quality the constructed image can achieve. Unfortunately, such theory is found not to be available in most existing techniques.

3) Even if it is possible to develop these techniques to be adaptable to the microwave imaging system (meaning that the first two problems are resolved), their performances are still not justified in considering the effect of low correlated source of microwave image and the additional cost and increasing complexity of hardware and software in applying these techniques.

The research objective was to develop a theory of Bit Compression for the high resolution microwave imaging system to determine the <u>minimum</u> number of bits required of the quantized signal for the image to achieve <u>any</u> given quality or, conversely, what quality of image can be obtained for <u>any</u> given number of bits that the quantized signal retains. The theory will be developed by 1) deriving an optimum quantization scheme which maximize the image quality over the entire system for given number of quantized level; 2) deriving a theoretically exact and physically solvable analytic relation between the number of bits per sample of the

quantized signal and the quality measure of image, and 3) analyzing the effects due to data compression.

2. THE THEORY

2-1 The System Model

A typical microwave imaging system model is shown in Figure 1 [5].

$S(r,\Theta)$ is a source distribution function which is actually a complex reflectivity function due to illumination from a distant microwave transmitter. The electric field e(x) induced in the aperture is related to $S(r,\Theta)$ by a diffraction integral. An angle Θ is measured from the normal to the aperture of the linear array. By replacing Θ with $u=\sin(\Theta)$, the integral transformation , for a far-field source or a near-field source with a well focused antenna array, is reduced to Fourier transform where u becomes the canonically conjugate variable to x/λ in the Fourier relation [4].

The source distribution $S(r,\Theta)$ can be reduced to one dimensional function $S_k(u)$ because the range dimension in radar can be considered as a discrete set of range bins indexed by k [5].

w(x) is the aperture weighting function. The current distribution f(x) in the aperture is the product of e(x) and w(x). With the exception of modern superresolution techniques [6], the image is generally the magnitude of the Fourier transform of the current distribution [5], which can be written as $I_f = | F(f) |$ where F(-) denotes Fourier transform.

When the data compression is introduced, the compressed aperture data becomes g=D[f] where D is the compression operator. The image reconstructed from compressed data then becomes the magnitude of the Fourier transform of g denoted by $I_g = |F(g)|$.

The selections of the weighting function w(x) will not change the nature of image distortion due to data compression because the reference image is I_f in which the effect of w(x) has been included.

Finally, the problem becomes that for a given image quality requirement of I_g, find a Bit Compression technique to compress f, such that the number of bits of g can be minimized.

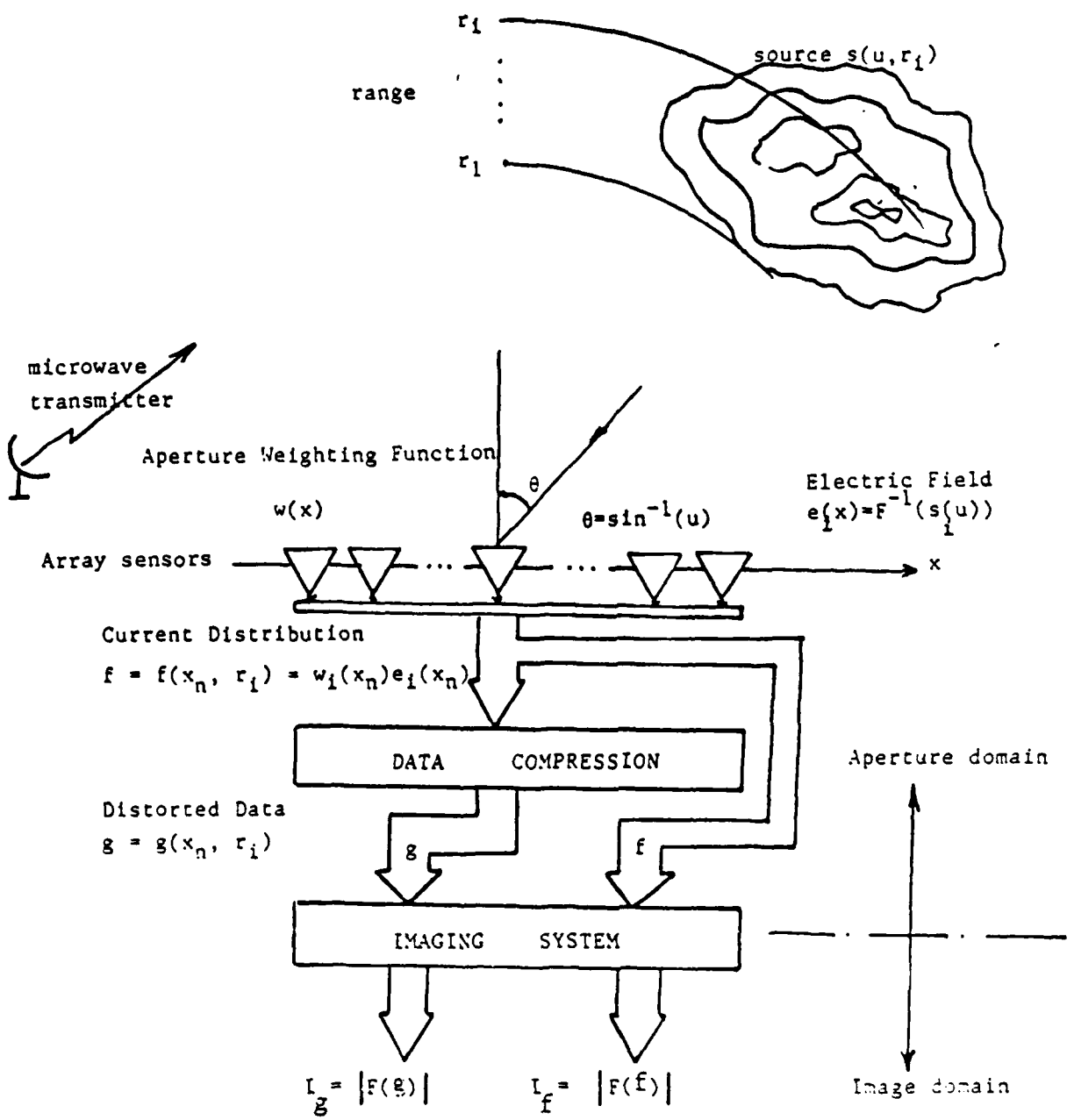

Figure 1. Microwave Imaging System Model

2.2 The Signal Model

The microwave image data can be considered as a random process. By definition, a random process is an ensemble of time functions where the time function is random variable for a given instant of time [7].

The random process model for microwave imaging is illustrated in Figure 2. For a given time instant which corresponds to one snap shot, the image data is the spatial sample of the radiation source for one range bin, therefore the time functions are the receiving signals in the aperture and the ensemble is defined to include all array elements.

The process is assumed to be ergodic because images corresponding to different snap shot are assumed to be uncorrelated.

The process is not stationary in general. However, the statistical study of data distributions shows that if scenes to be imaged are divided into different groups according to different categories of objects (e.g. residence, industrial, airplane,...,etc) then the process can be considered as stationary within a group provided that their data distributions are close enough and the parameters of the processor are not sensitive to variations of the data distributions in the group.

Therefore, it will be assumed that both the stationarity and the ergodicity are held for the model.

2.3 Basic Definitions

Image Fidelity Measure: Define the normalized zero-lag correlation coefficient ρ between the original and the distorted image as a measure of image quality:

$$\rho = \frac{\overline{I_f I_g}}{I_{frms} I_{grms}} \qquad (2.1)$$

where I_f denotes the original image and I_g denotes the image obtained from the distorted (i.e.,quantized) input data. Both

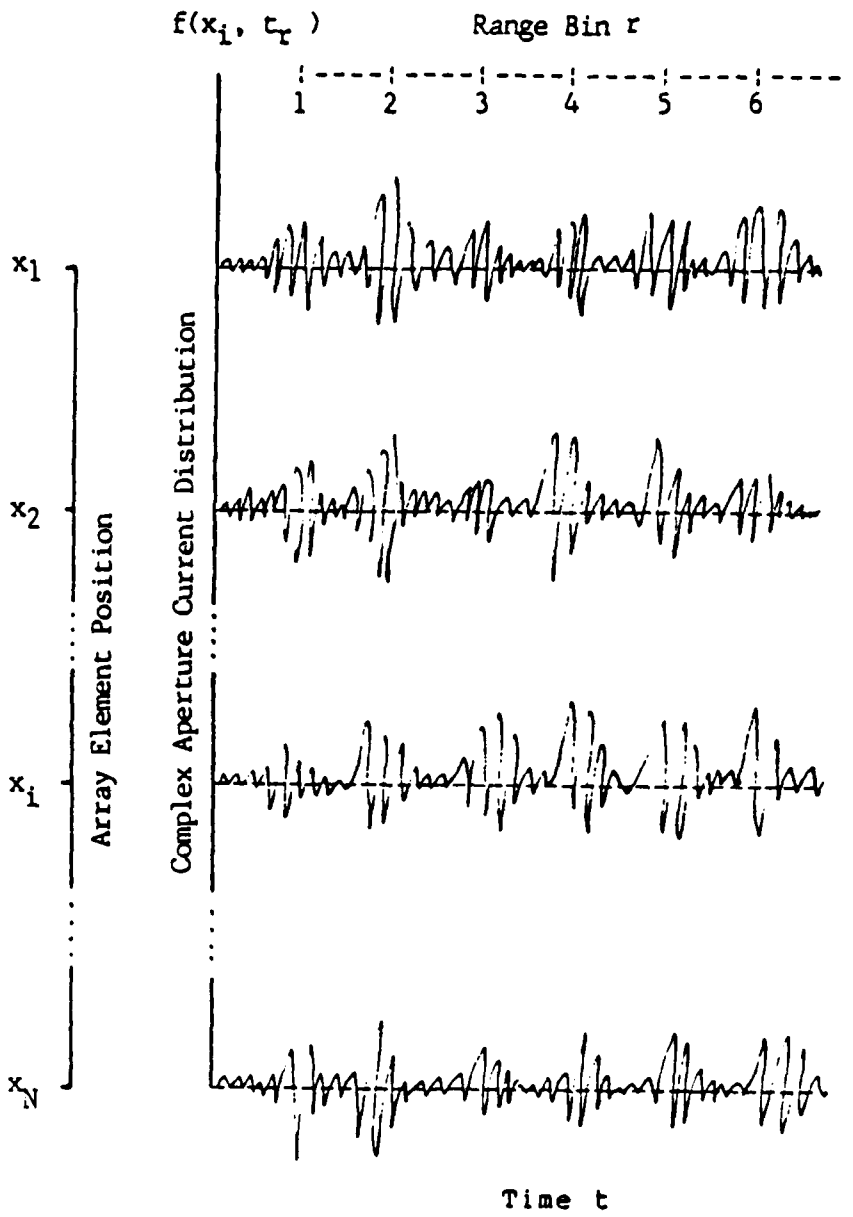

Figure 2. The Signal Model

I_f and I_g are functions of the image coordinates. The overbar means average over all picture elements in the images and rms denotes root mean square.

In most image processing applications, the mean square error ε is used to measure the image fidelity [1]. It has been shown [5] that ε and ρ are equivalent if ε is normalized and if the distorted signal g is scaled such that its energy and the energy of the original signal f are equal. However, these two major differences do make the correlation coefficient metric more useful in our application than the conventional mean square error metric. Because of the scaling property, the comparison between the proper image and the distorted image is made under the same energy base, so that only the unsimilarity will be detected from the measurement. Because of the normalization property, the sensitivity of the image quality measure to the variation of data distribution for different scene will be significantly reduced, and a bounded relative error scale will usually make more sense than an unbounded absolute error scale ε.

The selection of correlation coefficient metric become significant in the optimum quantization procedure where it leads to independent quantizer design while the mean square error metric lead to dependence between amplitude quantizer and phase quantizer.

Information Measure: Define entropy H to measure the information content of the quantized signals;

$$H_Z = -\sum_{i=1}^{N} p_{Zi} \log p_{Zi} \qquad (2.2)$$

where Z=A representing amplitude, Z=Ξ representing phase and p_{Zi} is the probability that the signal z takes a value in the ith quantization region .

2.4 Aperture Domain Formulation

We assume that the source or scene being imaged is in the far field. ρ can then be expressed in the aperture domain by

using the Fourier transform relationship between the source distribution and the electric field induced in the aperture, and Parseval's Theorem equating energies in the two Fourier domains [5]. In the following derivation, f consists of the measured samples of the electric field in the aperture and g are its values after quantization. f and g are functions of the aperture coordinates. $I_f=|F(f)|$ and $I_g=|F(g)|$. F(-) denotes Fourier Transform and * denotes the complex conjugate.

From (2.1),

$$\rho = \frac{\overline{I_f\, I_g}}{I_{frms} I_{grms}}$$

$$= \frac{\overline{|F(f)|\ |F(g)|}}{[\ F(f)\ ]_{rms}[\ F(g)\ ]_{rms}} .$$

Because

$$\overline{|F(f)|\ |F(g)|} \geq \left|\overline{F(f)\ F(g)^*}\right|$$

we write

$$\overline{|F(f)|\ |F(g)|} = K \left|\overline{F(f)\ F(g)^*}\right|$$

where K greater than or equal to 1. Then

$$\rho = K \frac{\left|\overline{F(f)\ F^*(g)}\right|}{[F(f)]_{rms}[F(g)]_{rms}}$$

$$= K \frac{\left|\overline{F(f)\ F^*(g)}\right|}{[\overline{|F(f)|^2}\ \ \overline{|F(g)|^2}\ ]^{1/2}}$$

Parseval's theorem implies that

$$\frac{\left|\overline{F(f)\,F^{*}(g)}\right|}{\left[\overline{|F(f)|^{2}}\;\;\overline{|F(g)|^{2}}\right]^{1/2}} = \frac{\left|\overline{f\,g^{*}}\right|}{\left[\overline{|f|^{2}}\;\overline{|g|^{2}}\right]^{1/2}}$$

Therefore

$$\rho = K\,\frac{\left|\overline{f\,g^{*}}\right|}{f_{rms}\,g_{rms}} \triangleq K\,\rho_{0} \qquad (2.3)$$

The analysis is performed in polar coordinates. Let $f=Ae^{j\Xi}$ and $g=A'e^{j\Xi'}$. Reference [5] shows phase and amplitude to be independent when the scene being imaged consists of many sources and none of the sources dominates all the rest. Assuming this condition, ρ_0 can be expressed as

$$\rho_{0} = \frac{\overline{A\,A'}}{A_{rms}A'_{rms}}\left|\overline{e^{j(\Xi-\Xi')}}\right|$$

$$= \rho_{A}\,\rho_{\Xi} \qquad (2.4)$$

where

$$\rho_{A} = \overline{A\;\;A'}/\,A_{rms}\,A'_{rms} \qquad (2.4a)$$

$$\rho_{\Xi} = \left|\overline{\exp\,(j(\Xi-\Xi'))}\right| \qquad (2.4b)$$

where the overbar means ensemble average over all array element which could be replaced by the expectation value because the number of array elements is very large.

2.5 Optimum Quantizer

Techniques of optimum quantization usually deal with real input sequences. Examples are the early papers by Max [8] and Paez and Glisson [9]. In high resolution microwave imaging, the aperture data to be quantized are complex random variables. In this thesis, an optimum quantization scheme for complex data in

polar coordinates is introduced . Gallagher [10] also dealt with optimum quantization of complex data in polar coordinates. There are two main differences between these two papers and this work.

First, in [8],[9] and [10], only the quantizer was optimized, whereas in our procedure, the optimization is carried out over the entire imaging system (which includes the transform from source distribution to electric field in the aperture and the inverse transform from quantizer output to image).

Second, the optimization procedure in [10] leads to an amplitude quantization scheme that is dependent upon the phase quantization. In our procedure, which maximizes the image correlation coefficient ρ (2.1), the amplitude and phase quantizer are independent . This is significant because 1) it gives the complete freedom to achieve the most efficent bit allocation between amplitude quantizer and phase quantizer; 2) it makes it possible to express the total entropy of the quantized signal with the individual entropy measurement from the two quantizers' output without involving conditional entropy [7] which is usually difficult to evaluate; and 3) it leads to a similar optimum conditions both for amplitude quantizer and phase quantizer as those developed for real signal by Max, so that one is able to use all resources and facilities developed for Max quantizer, such as Bruce's algorithm [11] and Sharma's algorithm [12], to calculate the optimum settings.

The conditions of optimum quantization will be obtained by maximizing the image correlation coefficient ρ.

It can be found later that the conditions which maximize ρ_0 also maximize K. Therefore, the image correlation coefficient ρ will be maximized as the lower bound correlation coefficient ρ_0 is maximized.

Because $\rho_0 = \rho_A \rho_\Sigma$, and because ρ_A and ρ_Σ are independent, ρ_0 is maximized as each of ρ_A and ρ_Σ is maximized individually.

2.5.1 Optimum Amplitude Quantizer

Let N_A be the number of quantized levels, a_i' be the ith output level of the quantizer, the value assigned to a sample

falling in the interval $[\, a_{i-1}, a_i \,)$, and a_i be the endpoint of input range of the quantizer with $i=1,2,\ldots,N_A$ (z replaced by a in Figure 3).

Define $\hat{a}_i = E(\, A \mid a_{i-1} \le A < a_i)$ with $E(-)$ representing expectation value, $p_{Ai} = Pr(\, a_{i-1} \le A < a_i)$ with $Pr(-)$ standing for probability,

The terms in (2.4a) may be calculated:

$$\overline{A\,A'} = \sum_i^{N_A} Pr(a_{i-1} \le A < a_i)\; E(\, AA' \mid a_{i-1} \le A < a_i)$$

$$= \sum_i^{N_A} p_{Ai} a_i'\; E(\, A \mid a_{i-1} \le A < a_i)$$

$$= \sum_i^{N_A} p_{Ai} a_i'\; \hat{a}_i$$

and

$$A'_{rms} = \left[\sum_i^{N_A} p_{Ai} E(A'^2 \mid a_{i-1} \le A < a_i) \right]^{1/2}$$

$$= \left[\sum_i^{N_A} p_{Ai} a_i'^2 \right]^{1/2}$$

The amplitude correlation coefficient is

$$\rho_A = \frac{\sum_i^{N_A} p_{Ai} a_i' \hat{a}_i}{\left[\sum_i^{N_A} p_{Ai} a_i'^2 \right]^{1/2} A_{rms}} \qquad (2.5)$$

It can be shown that ρ_A is maximized if a_i' and a_i satisfy

$$a_i' = \hat{a}_i \qquad i=1,2,\ldots,N_A \qquad (2.6a)$$

$$a_i = \frac{\hat{a}_i + \hat{a}_{i+1}}{2} \qquad i=1,2,\ldots N_A-1 \qquad (2.6b)$$

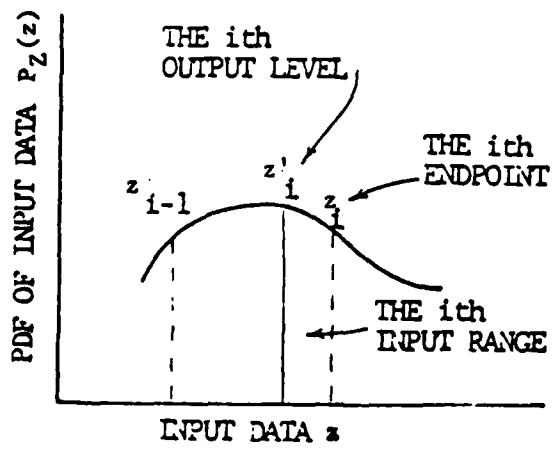

Figure 3. Description of Definitions of Quantizer Design

2.5.2 Optimum Phase Quantizer

Let N_{Φ} be the number of quantized levels, Φ_i' be the output level of the quantizer, the value assigned to a sample falling within the interval $[\Phi_{i-1},\Phi_i)$, and Φ_i be the endpoint of the input range of the quantizer with $i=1,2,\ldots,N_{\Phi}-1$ (z replaced by Φ in Figure 3).

Define $\hat{\Phi}_i = E(\Phi \mid \Phi_{i-1} \leq \Phi < \Phi_i)$ $E(\cdot)$ representing expectation value, and $p_{\Phi i} = Pr(\Phi_{i-1} \leq \Phi < \Phi_i)$ with $Pr(\cdot)$ standing for probability.

The phase correlation coefficient (2.4b) becomes

$$\rho_{\Phi} = \left| \overline{\exp[j(\Phi-\Phi')]} \right|$$

$$= \left| \sum_{i}^{N_{\Phi}} p_{\Phi i} E\{ \exp[j(\Phi-\Phi')] \mid \Phi_{i-1} \leq \Phi < \Phi_i \} \right|$$

It can be shown, for uniformly distributed phase, that ρ_{Φ} is maximized if Φ_i and Φ_i' satisfy:

$$\Phi_i' = \hat{\Phi}_i \qquad i=1,2,\ldots,N_{\Phi} \qquad (2.6c)$$

$$\Phi_i = \frac{\hat{\Phi}_i + \hat{\Phi}_{i+1}}{2} \qquad i=1,2,\ldots,N_{\Phi}-1 \qquad (2.6d)$$

Equations (2.6a)-(2.6d) are the design equations of the optimum quantizer. From (2.6), it is clear that the dependence between the amplitude quantizer and the phase quantizer in Gallagher's design vanishes. The equations (2.6a)-(2.6d) say that in the optimum design of the two quantizers, the ith output level equals the conditional mean of the input data in the ith range and the endpoint of the ith range equals the arithmetic mean of two adjacent output levels. These statements are true for arbitrary amplitude distribution, for uniform phase distribution and for amplitude and phase being independent.

2.6 The Transfer Index

From (2.1), one can see that ρ_0 has the same form as ρ except that it is defined as the magnitude of complex quantity. Therefore we can consider K as a transfer index which transfers the image correlation coefficient from the aperture domain into the image domain. The expression for K can be derived in the following procedure.

From (2.1),

$$\rho = \frac{\overline{I_f\, I_g}}{I_{frms} I_{grms}} = \frac{\overline{|F(f)|\ |F(g)|}}{[\ F(f)\ ]_{rms}[\ F(g)\ ]_{rms}}$$

But from (2.3)

$$\rho_0 = \frac{\left|\overline{f\, g^*}\right|}{f_{rms} g_{rms}} = \frac{\left|\overline{F(f)\, F^*(g)}\right|}{[F(f)]_{rms}[F(g)]_{rms}}$$

$$= C \left|\overline{|F(f)|\exp(j\phi_f)|F(g)|\exp(-j\phi_g)}\right|$$

where

$$C = \{\ [\ F(f)\ ]_{rms}[\ F(g)\ ]_{rms}\}^{-1}$$

Independence between phase and amplitude in the image domain [5] implies that

$$\rho_0 = C\ \overline{|F(f)|\ |F(g)|}\ \left|\overline{\exp(j(\phi_f-\phi_g))}\right|$$

$$= \left|\overline{\exp(j(\phi_f-\phi_g))}\right|\ \rho$$

which, by definition, gives

$$K = \left|\overline{\exp(j(\phi_f-\phi_g))}\right|^{-1}$$

Let A_i denotes the measured amplitude in the ith element, Ξ_i denotes the measured phase in the ith element, and " ' " represents values after distortion. After much mathematics, it is found that

$$K^{-1} = \left|\overline{\exp(j\alpha)}\right|$$

where

$$\alpha = \tan^{-1}\beta$$

and

$$\beta = \frac{(\Sigma\, A_i \sin\Psi_i)(\Sigma\, A_i' \cos\Psi_i') - (\Sigma\, A_i \cos\Psi_i)(\Sigma\, A_i' \sin\Psi_i')}{(\Sigma\, A_i \cos\Psi_i)(\Sigma\, A_i' \cos\Psi_i') + (\Sigma\, A_i \sin\Psi_i)(\Sigma\, A_i' \sin\Psi_i')} \tag{2.7}$$

where $\Psi_i = \Xi_i - \gamma_i$ with γ_i being the Fourier kernel, and the summation is taken over all elements (i from 1 to N).

By defining $\overline{V} \overset{\Delta}{=} N^{-1} \sum_i^N V_i$, β can be expressed as

$$\beta = \frac{(\overline{A \sin\Psi})(\overline{A'\cos\Psi'}) - (\overline{A \cos\Psi})(\overline{A'\sin\Psi'})}{(\overline{A \cos\Psi})(\overline{A'\cos\Psi'}) + (\overline{A \sin\Psi})(\overline{A'\sin\Psi'})} \tag{2.8}$$

Because the number of elements is very large, V can be approximated by the expectation value of X . This implies that the transfer index K is uniquely specified for given distribution of aperture data and the quantizer parameters as the number of elements goes to very large.

This property shows that the exact solution of image correlation coefficient exist if the distribution of aperture data are given. It also allow us to obtain K by using computer-simulated images through the relation $K=\rho/\rho_0$ with ρ obtained from (2.1) and ρ_0 obtained from (2.4). This method is more accurate than calculating (2.7) because of the tremendously reducing number of mathematical procedures that are involved; the result is smaller accumulation of errors in the calculation.

In section 2.5, it was shown that ρ_0 is maximized when the optimum quantization conditions are applied. A numerical study of (2.7) shows the same result for K, namely that K is maximized when the optimum quantization conditions are applied. Furthermore it was found that K is insensitive to changes in the output levels provided that the maximum deviation from the optimum set is less than 10 per cent.

Some values of the estimate of K are listed in Table 1.

A numerical study of K based on (2.7), and the results of experimental testing discloses the following additional important properties of K:

1) Using the estimates of K into the evaluation of image correlation coefficient with experimental data (Tables 5 and 6) infers that K is insensitive to variations in the distribution of the complex aperture data. This property is very important in a practical sense because it indicates that K is relatively scene free.

2) The transfer index K is more sensitive to phase distortion than to amplitude distortion. As Table 1 shows, K is closer to 1 for amplitude-distortion-only than for phase distortion.

3) The same table shows that when the phase distortion is significant (e.g., 1-2 bits of phase), K is determined almost entirely by the phase quantizer.

4) When the phase distortion is insignificant (e.g., 3 or more bits of phase), K is determined almost entirely by the amplitude quantizer.

2.7 The Analytic Equations

By applying the optimum condition (2.6) to (2.4) and summarizing the results from previous sections we obtain the analytic equations of image correlation:

$$\rho = K \rho_0$$

$$\rho_0 = \rho_A \rho_\Sigma$$

		H_Φ (bits)				
		1	2	≥ 3		
				R1	R2	
H_A (bits)	0	0.70	0.90	0.91	0.95	$\tilde{K}^{-1}$
	1	0.70	0.90	0.95	0.97	
	2	0.70	0.90	0.97	0.99	

Table 1. Estimate of K^{-1}. The ranges R1 and R2 defined by R1:$(0.6 \leq \rho_A^* \leq 0.9)$ and R2:$(0.9 \leq \rho_A^* \leq 1.0)$ where $\rho_A^* = \bar{A}/A_{rms}$

$$\rho_A = \hat{a}_{rms}(a_i)/A_{rms} \qquad (2.9a)$$

where $\hat{a}_{rms} = \left[\sum_{i=1}^{N_A} p_{Ai} \hat{a}_i^2 \right]^{1/2}$

$$\rho_\Xi = \mathrm{sinc}(\pi\, 2^{-H_\Xi}) \qquad (2.9b)$$

$$H_Z(z_i) = - \sum_{i}^{N_Z} p_{Zi}(z_i) \log p_{Zi}(z_i)$$

where Z=A representing amplitude and $Z=\Xi$ representing phase.

The independence between the amplitude quantizer and phase quantizer implies

$$H = H_A + H_\Xi$$

K is determined by

$$K = \left| \overline{\exp(j\alpha)} \right|^{-1}$$

where

$$\alpha = \tan^{-1}\beta$$

and

$$\beta = \frac{(\overline{A \sin\Psi})(\overline{A'\cos\Psi'}) - (\overline{A \cos\Psi})(\overline{A'\sin\Psi'})}{(\overline{A \cos\Psi})(\overline{A'\cos\Psi'}) + (\overline{A \sin\Psi})(\overline{A'\sin\Psi'})}$$

For given system constraints, this set of equations relates the optimum image quality to the minimum number of bits per sample of the quantized signal through the optimum endpoints setting $\{z_i\}$ and optimum output levels $\{\hat{z}_i\}$

Table 2 lists some results of exact image correlation coefficient ρ versus the number of bits per sample in amplitude and phase for Rayleigh distributed amplitude and uniformly distributed phase which shows that the image quality is well

		H_ϕ(bits)			
		1	2	3	
H_A (bits)	0	0.806	0.886	0.949	$\rho=K\rho_o$
	1	0.873	0.961	0.985	
	2	0.896	0.986	0.990	

Table 2. Image Correlation Coefficient vs. the number of Bits Per Sample: Amplitude and Phase

preserved for high compressed aperture data (for example, from the first column first row of Table 2, one can see that more than 80% of the image fidelity is achieved for only 1 bit of aperture data).

As one can observe that both the analytic equations of image quality and the optimum conditions have no closed-form solution. They can only be solved numerically by using large computer program. However, in order to study the properties of the theory, it is not always necessary to carry out the general and exact solutions. Good approximation and simulation using typical distribution are usually more desirable.

2.8 Suboptimum Conditions

It is well known that phase carries more information useful for image construction than amplitude. Therefore, a suboptimum amplitude quantization schemes could yield near-optimum results provided the phase is optimally quantized.

If one replaces the condition of (2.6b) with the condition of setting all p_{Ai} to be equal:

$$p_{Ai} = p = 2^{-H_A} \qquad \text{for all } i \tag{2.10}$$

then the quantization procedure can be reduced to one dimensional and P_A can then be expressed explicitly as the function of H_A

$$P_A = \left[2^{-H_A} \sum_{i=1}^{2^{H_A}} \hat{C}_i^2(H_A) \right]^{1/2} \tag{2.11}$$

where

$$\hat{C}_i = \hat{a}_i / A_{rms}$$

Because $\hat{C}_i$ is only a function of H_A , P_A is uniquely specified by H_A.

It is found by computer calculation of (2.9a) and (2.10) that ρ_A(2.9a) is almost identical to ρ_A(2.10) in the sense that the largest error between them, which appears when N_A=2, is less than 0.2%. However, equation (2.10) greatly simplifies the analysis procedure.

2.9 Simulation

Assuming that the scene to be imaged is in the far field and consist of many sources (targets) characterized by a real amplitude A_i and phase θ_i, the electric field induced in the antenna array is $e(x) = \Sigma A_i \exp(jkxu_i + \theta_i)$. Further assuming that none of the sources dominates the sum of all the rest which suggests that all these sources are independently identically distributed. By the Central Limit Theorem, the quadrature components of the electric field are independent Gaussian processes which implies that the amplitude and the phase of the current distribution f are independent with Rayleigh distributed amplitude and uniform distributed phase. By using this multiple targets model [5] and applying the suboptimum condition (2.10), a closed form solution of lower bound image correlation coefficient ρ_O in terms of the entropy of quantized signal can be obtained.

To see this, recall equation (2.11)

$$\rho_A = (2^{-H_A \Sigma \hat{C}_i^2})^{1/2}$$

where

$$\hat{C}_i = \hat{a}_i / A_{rms}$$

with

$$p_{Ai} = p = 2^{-H_A} \text{ for all } i.$$

By Noting that the pdf of amplitude is Rayleigh, that is

$$P_A(a) = (a/\sigma^2)\exp(-(a^2/2\sigma^2))$$

Evaluating the terms in (2.11) gives

$$A_{rms} = (\int_0^\infty a^2 P_A(a)\, da)^{1/2} = \sqrt{2}\,\sigma \qquad (2.12)$$

where σ is the standard deviation of amplitude.

$$\hat{a}_i = E(A \mid a_{i-1} \leq A < a_i) = p^{-1} \int_{a_{i-1}}^{a_i} a\, P_A(a)\, da$$

$$= p^{-1}\{-a_i \exp(-a_i^2/2\sigma^2) + a_{i-1}\exp(-a_{i-1}^2/2\sigma^2)$$

$$+ \sqrt{2\pi}\,\sigma\,[\mathrm{Erf}(a_i/\sigma) - \mathrm{Erf}(a_{i-1}/\sigma)]\} \qquad (2.13)$$

where Erf(x) is the error function of x defined by

$$\mathrm{Erf}(x) = (\sqrt{2\pi})^{-1} \int_{-\infty}^{x} \exp(-y^2/2)\, dy$$

After much mathematics, a_i is found to be:

$$a_i = \{2 \ln[(1-ip)^{-1}]\}^{1/2}\sigma \quad i=0,1,\ldots,N_A-1 \qquad (2.14)$$

and

$$a_{N_A} = \infty$$

Now let

$$C_i = a_i / [(\pi/2)^{1/2}\sigma] \qquad (2.15)$$

and note that

$$p = 2^{-H_A} = N_A^{-1}.$$

then

$$C_i = 2\{\ln[(1-i2^{-H_A})^{-1}]/\pi\}^{1/2} \quad i=0,1,\ldots,N_A-1 \qquad (2.16)$$

Substitute (2.15) into (2.13) and then substitute the modified (2.13) and (2.12) into $\hat{C}_i$ in (2.11). The result is

$$\hat{C}_i = 2^{H_A}\sqrt{\pi}\,\{0.5\,[\,C_{i-1}\exp(-\pi C_{i-1}^2/4) - C_i \exp(-\pi C_i^2/4)]$$

$$+[\,\mathrm{Erf}(C_i(\pi/2)^{1/2}) - \mathrm{Erf}(C_{i-1}(\pi/2)^{1/2})]\}$$

(2.17)

where $i=1,2,\ldots,N_A-1$, and C_i is determined by (2.16).

A summary of results follows:

$$\rho_O = \rho_A \rho_\Sigma$$

$$H = H_A + H_\Sigma$$

$$\rho_A = \left[2^{-H_A} \sum_{i=1}^{2^{H_A}} \hat{C}_i^2(H_A) \right]^{1/2}$$

where

$$\hat{C}_i = 2^{H_A} \sqrt{\pi} \{ 0.5 [C_{i-1}\exp(-\pi C_{i-1}^2/4) - C_i \exp(-\pi C_i^2/4)] + [\mathrm{Erf}(C_i(\pi/2)^{1/2}) - \mathrm{Erf}(C_{i-1}(\pi/2)^{1/2})]\}$$

$$C_i = 2 \{ \ln[(1-i2^{-H_A})^{-1}]/\pi\}^{1/2} \quad i=0,1,\ldots,N_A-1$$

ρ_A can be approximately given by

$$\hat{\rho}_A = 1-\exp[-(1.056H_A^{0.95}+2.173)]$$

Lastly

$$\rho_\Sigma = \mathrm{sinc}(\pi\, 2^{-H_\Sigma})$$

Results from carrying out these equations are shown in Table 3, Table 4, Figure 4 and Figure 5. Table 3 lists ρ_O for various combinations of H_A and H_Σ. Table 4 relates the correlation coefficient ρ_O to a subjective assessment of image quality [5]. Figure 4 plots ρ_A and ρ_Σ against the number of amplitude and phase bits per sample and Figure 5 plots ρ_O where the dashed lines are for constant sums of H_A and H_Σ.

An Important observation drawn from the analytic equations ((2.11)-(2.17)) of lower bound correlation coefficient ρ_O is that ρ_O is independent with the statistical properties (mean or variance) of the image data and uniquely related to the entropies

ρ_e H_A \ H_ϕ	0	1	2	3	4	5	6	7
0	0.0000	0.5541	0.7978	0.8636	0.8805	0.8848	0.8858	0.8861
1	0.0000	0.6114	0.8646	0.9359	0.9542	0.9588	0.9600	0.9603
2	0.0000	0.6272	0.8870	0.9601	0.9789	0.9836	0.9848	0.9851
3	0.0000	0.6330	0.8952	0.9689	0.9879	0.9927	0.9939	0.9942
4	0.0000	0.6352	0.8983	0.9723	0.9913	0.9961	0.9973	0.9976
5	0.0000	0.6360	0.8995	0.9736	0.9926	0.9975	0.9987	0.9990

Table 3. ρ_e vs number of bits per sample: amplitude and phase

ρ_e	Image
0.6	often recognizable
0.8	often acceptable
0.9	good quality
0.99	high fidelity

Table 4. Experimental relation of correlation to image quality

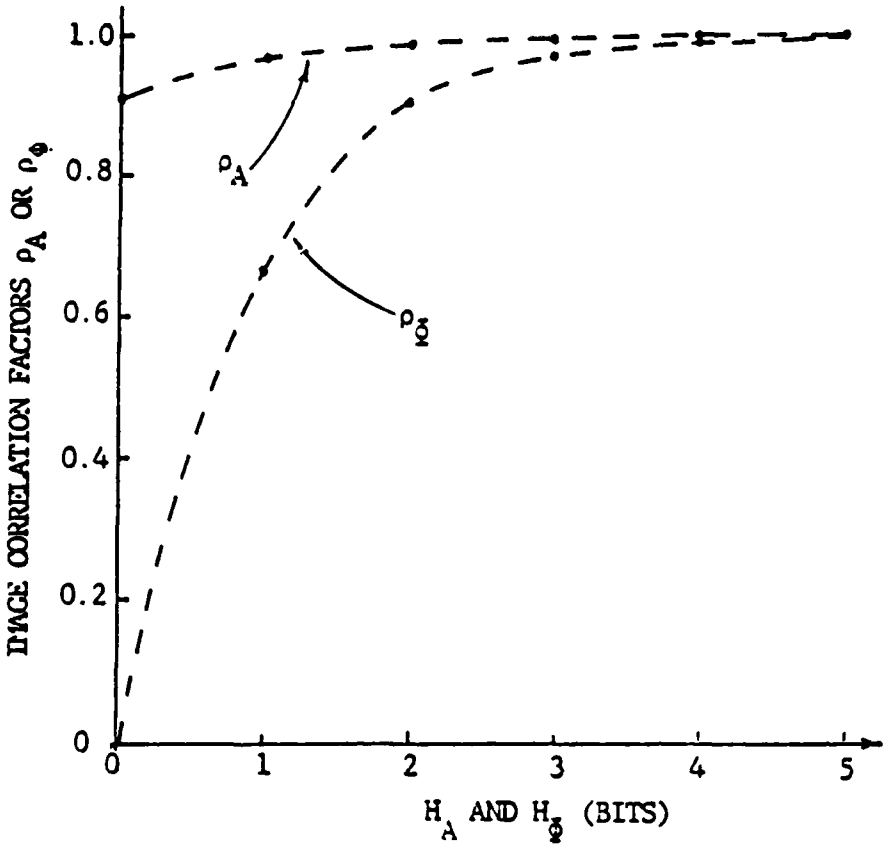

Figure 4. ρ_A vs. Number of Amplitude Bits Per Sample and ρ_Φ vs. Number of Phase Bits Per Sample

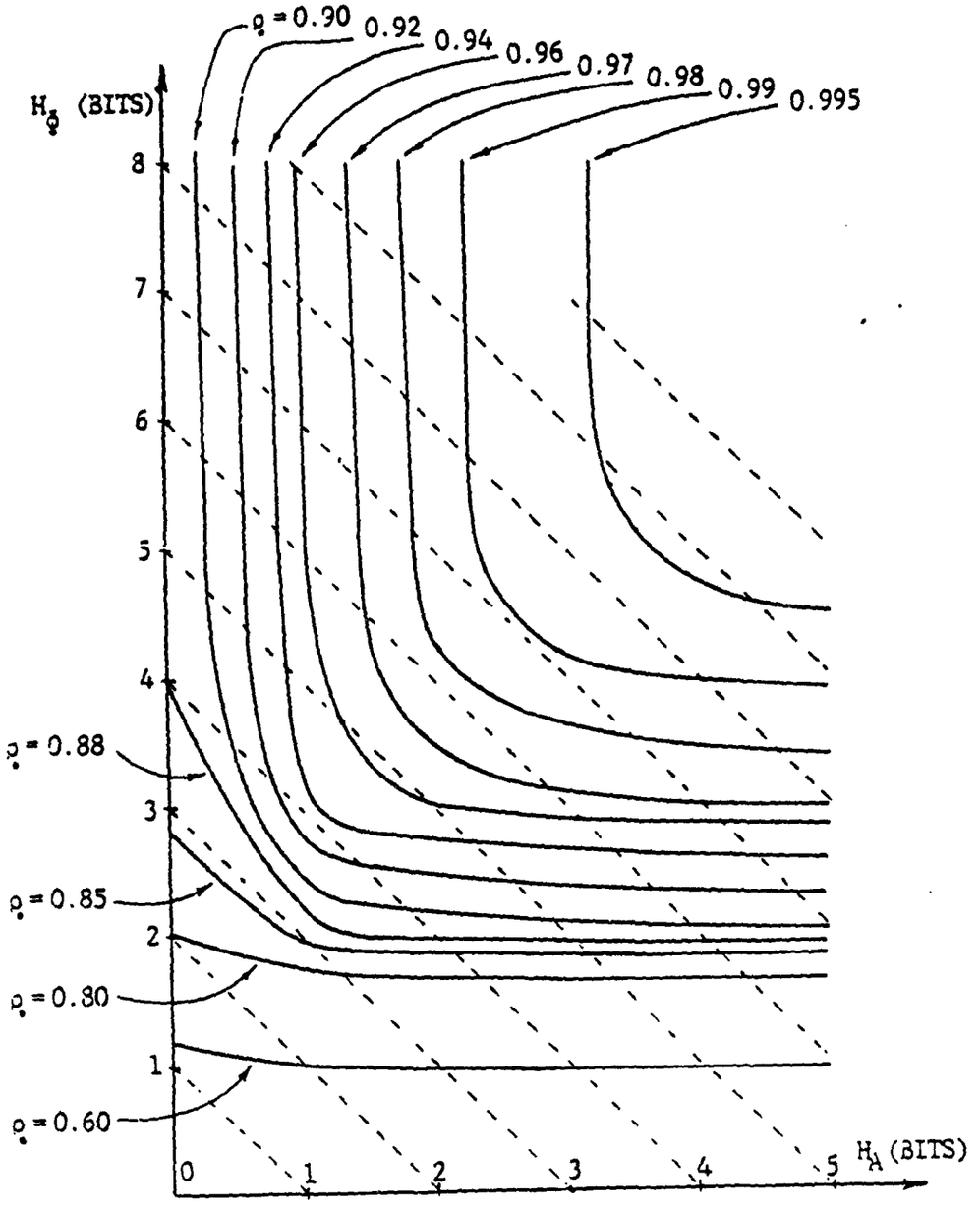

Figure 5. Lower Bound Correlation Coefficient ρ_0 As a Function of The Number of Amplitude Bit H_A and Phase Bits H_ϕ Per Sample

of the quantized signals. This conclusion can also be considered as correct for the exact image correlation coefficient ρ because the transfer index K, when the number of phase bits is small, is asymptotically independent with amplitude which is the one being the function of mean and variance.

It is shown that the phase carrying more information useful for image construction than amplitude. This can be seen in Figure 4 which shows that ρ_{Σ} dominates the value of ρ_{O}.

It is also shown that hard-limiting the input signals to a phased array while leaving the phase unaltered preserves much of the image integrity. This agrees with work by Kermish [15], Van Hove [16] [17], Oppenheim [18], and Steinberg [5]. The result is seen in Figure 5 on the upper portion of the H_{Σ}axis (H_A=0): the correlation coefficient ρ_{O} in this region is nearly 0.9 indicating (Table 4) good image quality. Amplitude-only information,on the other hand, destroys the image. Hard limiting plus one bit of phase information sometimes suffices (ρ_{O}= 0.6). Hard limiting plus two bits of signal phase per sample results in a correlation coefficient of 0.8, which often results in acceptable imagery.

Figure 5 shows that a minimum of four bits of information per complex signal sample guarantees a relatively good image ($\geq$0.9) provided that three bits are used for the phase and one bit for the amplitude. Eight bits are required to ensure a high fidelity image ($\geq$0.99).

Table 3 and Figure 5 provide a quantitative rule of thumb for assigning data bits to phase and amplitude: When the number of bits per data sample, $H_A + H_{\Sigma}$, is no more than 8, the number of bits assigned to phase should be two larger than the number of bits assigned to amplitude. When $H_A + H_{\Sigma} \geq 10$, $H_A = H_{\Sigma}$ is the optimum assignment. These rules also show that the phase information thoroughly dominates the process which is again agree with the well known experimental results in coherent imaging (e.g. holography or microwave imaging).

3. EXPERIMENTS

We have conducted 6 experiments to test the theory. The experimental data are obtained from near-field two-dimensional high-resolution radio camera images having 3m of range resolution and 2-6m cross-range resolution [2]. The wavelength is 3cm. The experiment numbers and the target descriptions are as follows:

301	Limerick Nuclear Power Plant
303	Cromby Power Plant
308	Marshall Street, Residential Houses
309	High Street, Residential Houses
310	Potato-Chip Factory
312	Suburban Housing Development

The targets are all in Phoenixville,PA, at distances of 4.5 to 17 km from the radio camera, which is located at the Valley Forge Research Center of the University of Pennsylvania. The image correlation coefficient obtained from the experimental data is denoted by ρ_x which is obtained by evaluation of (2.1) using images produced by experimental data with optimum quantization applied.

The value predicted by the theory is $\rho=K\rho_0$ where ρ_0 obtained by (2.9a) and (2.9b) using measured data in the aperture and K is obtained from Table 1.

3.1 Phase Distortion Only Experiments

In this case $\rho=K\rho_\Sigma$ because $\rho_A=1$. ρ_Σ was directly calculated from (2.9b). The comparison between ρ_x and ρ for the six experiments are shown in Table 5. The seventh row shows the average of the measured correlation coefficients of the experimental data. In the eighth row are the predicted values.

From Table 5 one can observe that the theoretical value is very close to the average experimental value. This is a highly practical result because the theoretical correlation (2.9b) was derived under the assumption of uniformly distributed phase. In

	run	1 bit of phase	2 bits of phase	Remarks
ρ_x	301	0.89	0.98	Experimental correlations
	303	0.92	0.98	
	308	0.91	0.98	
	309	0.90	0.98	
	310	0.92	0.98	
	312	0.93	0.98	
$\bar{\rho}_x$		0.91	0.98	Ave. exp.correl.
$\rho=K\rho_o=K\rho_\phi$		0.91	0.99	Theoretical value

Table 5 ρ_x Compared with ρ. Phase Distortion Only

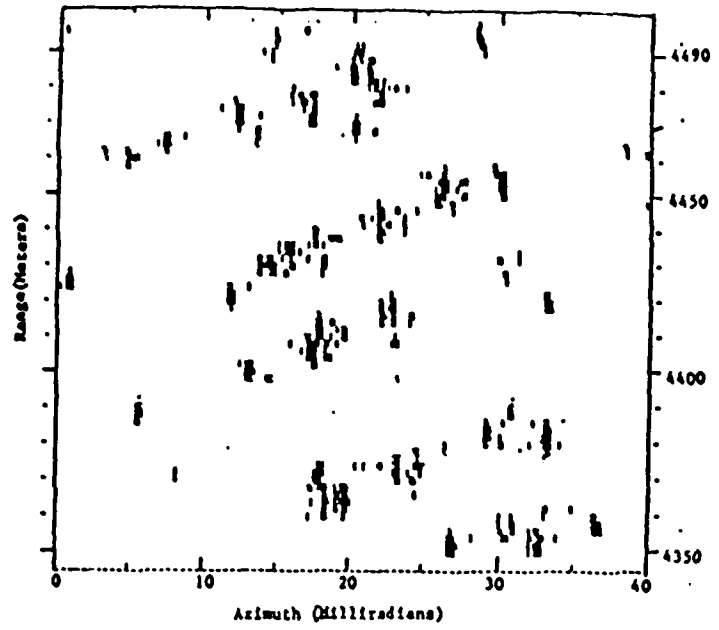

Image of Housing Development(R312)

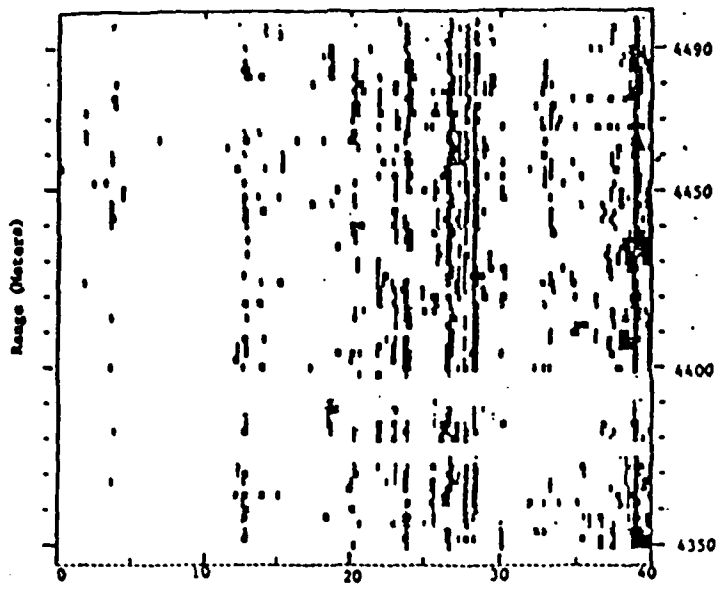

Image of Housing Development without Phase Information

Figure 6. Image of Run 312 without Phase Information

actuality, the real phase distributions, obtained by study of the phase histograms, are not quite uniform and are distinguishably different from scene to scene. This means that ρ is insensitive to variations in the distribution of phase.

The value of ρ for the 'no phase' case turns out to be indeterminate because (2.8), from which K is determined, become indeterminate. It was shown experimentally in [5] that no-phase data produce a meaningless image (Figure 6). It is for this reason that this case is ignored in Table 5.

3.2 Amplitude Distortion Only Experiments

In this case $\rho=K\rho_A$ because $\rho_\Sigma=1$. The theoretical values are given in the left column of each group of data in Table 6. K was obtained from Table 1. ρ_A was calculated from (3.3) in which A_{rms} and the $\hat{a}_i$ were estimated from the individual data sets.

The second column is ρ_x.

The third column is ρ'_x, which is obtained from images produced with the optimum quantizer design based on the assumption that each distribution was Rayleigh.

Four observations can be drawn form Table 6:

1) The values of ρ predicted by the theory are very close to ρ_x obtained from the images.

2) Unlike what was observed in the phase-distortion-only experiment, the image correlations are remarkable different from scene to scene specially when the number of amplitude bits is small (e.g., for hardlimiting, $\rho_{301}=0.69$ while $\rho_{308}=0.89$, and all of them are significantly smaller than the image correlation obtained from Rayleigh distributed amplitude data, which is $\rho=0.94$). One can also see that image correlation coefficients are similar when their amplitude histograms are similar. (e.g.,data sets of runs 309 and 310 and of 308 and 312.) If we define the image point occupancy to indicate the "mass" of the image:

$$I_o \triangleq \overline{I_f} \;/\; I_{frms} \qquad (3.1)$$

run	H_A(bits)								
	0			1			2		
	$\rho=K\rho_A$	ρ_x	ρ'_x	$\rho=K\rho_A$	ρ_x	ρ'_x	$\rho=K\rho_A$	ρ_x	ρ'_x
301	0.70	0.70	0.69	0.80	0.81	0.84	0.88	0.90	0.89
303	0.79	0.77	0.77	0.92	0.91	0.92	0.97	0.97	0.96
308	0.88	0.89	0.89	0.95	0.95	0.95	0.96	0.97	0.97
309	0.78	0.79	0.79	0.89	0.89	0.91	0.93	0.95	0.95
310	0.80	0.81	0.81	0.92	0.90	0.91	0.95	0.95	0.94
312	0.85	0.86	0.86	0.93	0.94	0.94	0.96	0.97	0.96
Rayleigh	0.95	0.94	0.94	0.99	0.98	0.98	0.99	0.99	0.99

Table 6. ρ_x Compared with ρ. Amplitude Distortion Only. ρ is the image correlation predicted by the theory. ρ_x and ρ'_x are the measured correlations when the quantizer design was optimized for each measured aperture distribution, and for the Rayleigh distribution, respectively. The values in the bottom row are based on simulation data having a Rayleigh distribution.

which is the normalized mean value of image, or more imaginally the image correlation between the image and a homogeneous black image (hardlimiting image). The results of ρ versus I_o are tabulated in Table 7. From Table 7, one can see that ρ increases toward the theoretical value as I_o increases.

3) It is evident that the estimates of K from Table 1 which are used to evaluate ρ in Table 6 work quite well for all scenes although all of them have different amplitude distributions. This means that K is nearly a scene-free parameter.

4) A very important observation from the comparison of ρ_x and ρ_x' is that the quantizer design based on the Rayleigh distribution gives nearly identical performance , in almost all cases, to the designs using the six actual distributions. This implies that one quantizer design is appropriate for all scenes.

run #	ρ_x(Hardlimiting)	I_o
301	0.70	0.37
303	0.77	0.42
309	0.79	0.42
310	0.81	0.50
312	0.86	0.55
308	0.89	0.58

Table 7. ρ_x vs. Image Points Occupancy

4. DISCUSSION AND CONCLUSION

4.1 Practical Considerations

Observations drawn from the experimental testing of the theory can be summarized into the following categories with practical considerations, and two major aspects of the theory, which are the optimum quantizer design and the estimate of image correlation coefficient, will be examined.

1)Sensitivity: The qualitative analysis and numerical study shows that the transfer index K is insensitive to the amplitude distribution and to the variation in phase distribution, while Table 6 shows that P_0 is relatively sensitive to the changes of amplitude distribution. The optimum quantizer design is found not sensitive to the data distributions.

2)Generality: The theory was developed under the assumption of a uniform distribution of phase in the aperture data; no restriction was imposed upon the amplitude distribution. However, since the variation from uniform distribution that the phase distributions of actual data have is considered as small and both optimum quantization conditions and estimate of ρ are insensitive to the phase variations. The theory is practically general.

3)Scene Independence: The insensitivity of data distributions implies nearly scene-free performance of the optimum quantizer. The estimate of ρ is not a scene-free quantity in general. However, if we classify scenes into different groups according to the nature of the scene (e.g. industrial, residence, field or airplane, etc) or the image points occupancy of the scene, then, within a group, the amplitude signal can be considered as stationary and the scene dependence of ρ can be eliminated. Under this condition, the theory can be consider as scene-free.

4) Capability of real-time processing: In many image processing situations, real-time processing is preferred. The optimum design requires knowledge of the statistical properties of the input data which, in principle, requires that data be acquired

and analysed. Such a process precludes real-time operation. However, the nearly scene-free performance observed in this study allows the designer to avoid the distribution-estimation steps and to base the design upon assumptions of uniform phase and Rayleigh amplitude distributions. By making these priori assumptions regarding the data, the quantizing operation becomes real-time.

4.2 Distortion Analysis

Knowledge about distortion so far is limited to knowing how much percent of the energy belongs to distortion. It is not sufficient. In order to determine the tolerance to distortion in the image, one has to know how the error energy is distributed. In other words, is it randomly and homogeneously distributed over all place? or does it build up coherently? If false targets are created, how do they relate to the data compression procedure and to the original image, etc..

Some earlier research on the nature of image distortion from hardlimiting aperture data have shown that the hardlimiting procedure does produce false targets (ghosts) [4], [13]-[14]. It is also found that the distorted image is related to the original image by some kinds of convolution relationship [4] [15].

A complete solution to this problem is out of the scope of this work. However, a procedure is developed here to give some useful guidelines to approach the solution.

By assuming that

$$f = Ae^{j\Xi} = \sum_i A_i e^{j\Xi_i} \delta(x - x_i) \qquad (4.1)$$

$$g = A'e^{j\Xi'} = \sum_i A_i' e^{j\Xi_i'} \delta(x - x_i) \qquad (4.2)$$

and letting

$$K_{Ai} = A_i'/A_i \ , \text{ and } \quad K_{\Xi i} = \Xi_i' / \Xi_i$$

we have

$$g = \sum_i A_i' e^{j\Xi_i'} \delta(x - x_i)$$

$$= \sum_i K_{Ai} A_i e^{jK_{\Xi i}\Xi_i}\, \delta(x - x_i)$$

$$= \sum_i K_{Ai} e^{j(K_{\Xi i} - 1)\Xi_i}\, A_i e^{j\Xi_i} \delta(x - x_i)$$

$$= [\sum_i K_{Ai} e^{j(K_{\Xi i} - 1)\Xi_i} \delta(x - x_i)]$$

$$[\sum_k A_k e^{j\Xi_k} \delta(x - x_k)]$$

$$= [\sum_i (A_i' / A_i)\, e^{j(\Xi_i' - \Xi_i)}\, \delta(x - x_i)]$$

$$[\sum_k A_k e^{j\Xi_k} \delta(x - x_k)]$$

$$= [(A' / A)\, e^{j(\Xi' - \Xi)}][A\, e^{j\Xi}]$$

$$= H_d\, f$$

therefore

$$\dot{I}_g = h_d * \dot{I}_f \qquad (4.3)$$

where

$$\dot{I}_g = F(g),\ h_d = F(H_d) \text{ and } \dot{I}_f = F(f)$$

$$I_g = |\dot{I}_g|,\ I_f = |\dot{I}_f|$$

One can see that the distortion process has the same form as a linear filtering process with filter transfer function

$$H_d = (A'/A)\, e^{j(\Xi' - \Xi)} \qquad (4.4)$$

except that the parameters of H_d are discrete random variables.

Let the complex image

$$\dot{I}_f = \sum_i F_i \, \delta(u-u_i)$$

where $u_i = \sin(\Theta_i)$ represents the ith pixel location in a given range bin and F_i represent the complex pixel value at that position . Then the complex distorted image $\dot{I}_g$ can be expressed as

$$\dot{I}_g = \dot{I}_f * h_d$$

$$= [\sum F_i \, \delta(u-u_i)] * h_d$$

$$= \sum F_i \, h_d(u-u_i)$$

which shows that the distortion operation is equivalent to the procedure that first shifts h_d to every pixel location multiplied by the pixel value at that position, and then adds them together over the entire image field.

From here, one can immediately observe that

1) the distortion energy will be spread all over the image plane;

2) the nature of the ghosts depends very much on the tail structure of h_d.

Therefore, as a guideline of distribution analysis, the shade of h_d will be investigated for various case of data compression.

4.2.1 Effect of Amplitude Distortion

For amplitude distortion only, we have

$$H_d = A'/A \qquad (4.5)$$

For the case of no distortion, $H_d = 1$. The "filter" is indeed an all-pass filter.

As the number of quantized level decrease, the fluctuation range of H_d ,in which 99 per cent of the data points of H_d are

located, and the fluctuation rate (rate of changes in amplitude from two adjacent elements) increase, so that more tail structures are added to h_d in the image domain according to the property of Fourier transform (Figure 7). The probability of getting false targets is therefore increased. In the case of hardlimiting (0 bit of amplitude), the fluctuation range reach its maximum. Because the large part of tail structure of h_d is in small magnitude, and because any pixel value which is lower than certain threshold (usually -20dB) will be considered as background noise, the major effect of amplitude distortion is to increase the noise level as well as to decrease the dynamic range.

4.2.2 Effect of Phase Distortion

For phase distortion only, we have

$$H_d = \exp(\Xi' - \Xi)$$

$$= \exp(\delta\Xi) \tag{4.6}$$

$$h_d(u) = N^{-1} \sum_{i}^{N} \exp[-j(\delta\phi_i + \gamma_i(u))$$

$$= N^{-1} \sum_{i}^{N} \exp[-j(\Psi_i(u))] \tag{4.7}$$

where γ_i is the Fourier Kernel.

Equation (4.7) can be considered as a summation of unit vectors with angle Ψ_i.

Let us first consider two extreme cases:

For the case of no distortion, H_d=1, h_d becomes a δ function as expected.

For the case of no-phase distortion (Ξ'=0, $\delta\phi_i = -\phi_i$),

$$h_d(u) = N^{-1} \sum_{i}^{N} \exp[-j(\phi_i + \gamma_i(u)) = 0$$

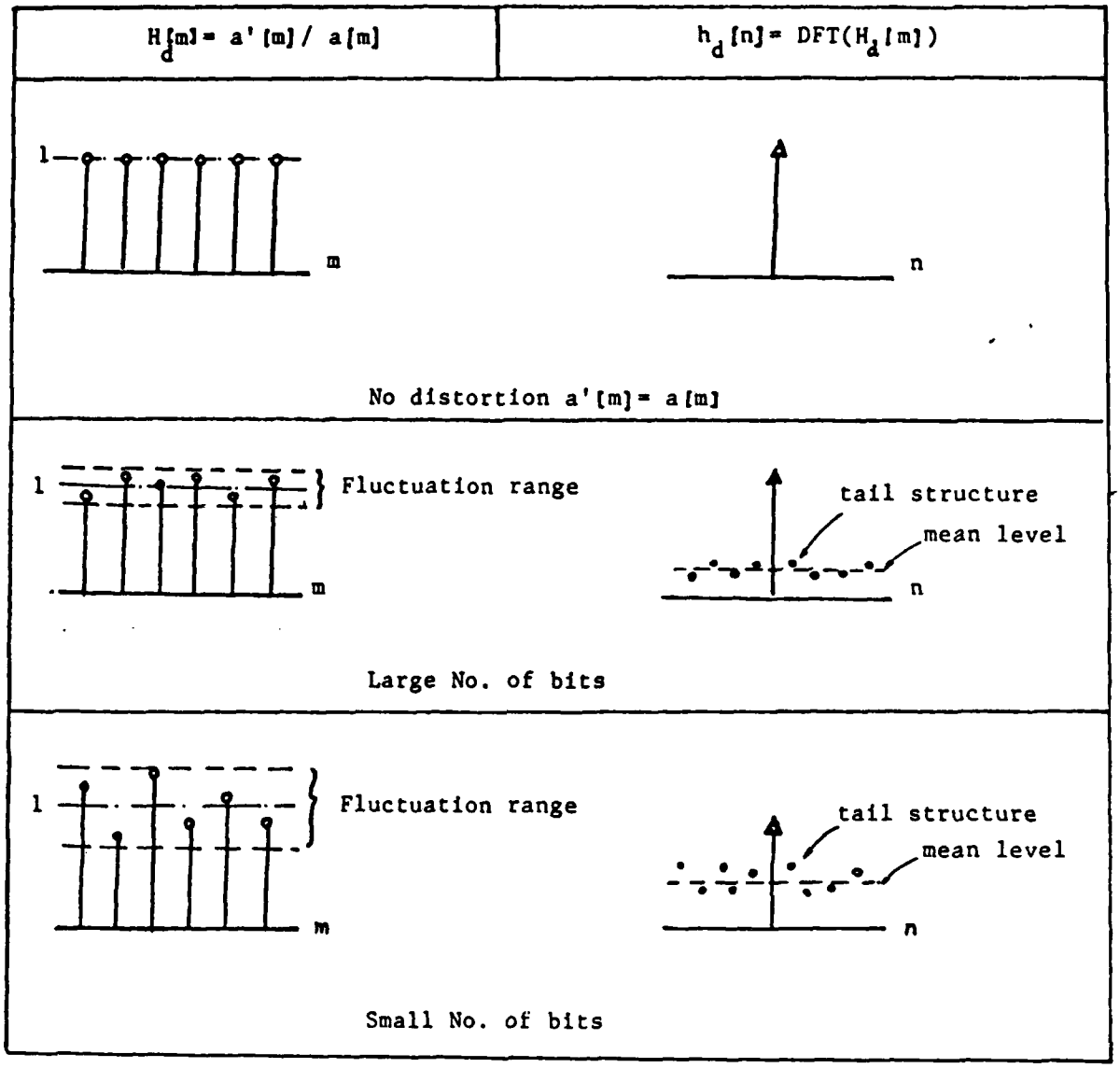

Figure 7 . Illustration of Analysis of h_d for Amplitude Distortion

as N goes to infinity. all vectors are canceled out include broadside because ϕ_is so as Ψ_is are uniformly distributed over 0 to 2π for all u. It follows that $\dot{I}_g = h_d * \dot{I}_f = 0$ and $I_g = |\dot{I}_g| = 0$, which lead to an undetermined value of ρ. For N being finite, this summation might not be zero. However, as shown in Figure 6, it does result in a meaningless image.

When more distortion is introduced (the number of bits decreases), the fluctuation range and the fluctuation rate of the projections of the unit vectors H_{di} on both the real axis and imaginary axis increases (Figure 8). As the same consequence as for amplitude distortion, more tail structure are added onto h_d. Therefore, the major effect due to phase distortion is basically the same as in the case of amplitude distortion.

The above analysis provide us a roughly picture about how the distorted energy will distributed and give guideline for further study on the subject. Although the distorted image I_g is defined as the magnitude of $\dot{I}_g$ and h_d is a complex quantity, the analysis on the structure of $|h_d|$ will still be very valuable to the analysis of false targets distribution because

$$I_g = |\dot{I}_g|$$

$$= | \Sigma F_i \, h_d(u-u_i) |$$

$$\leq \Sigma |F_i| \, |h_d(u-u_i)|$$

which means that the result from the analysis on $|h_d|$ gives the information upon the upper bound of the false targets distribution. In other words, the actual result will never be worse than the result from the analysis.

4.3 Conclusions

Summarizing results obtained from the previous sections, we conclude:

1) Image quality is measured by image correlation coefficient ρ defined by (2.1). It can be expressed in the aperture domain as

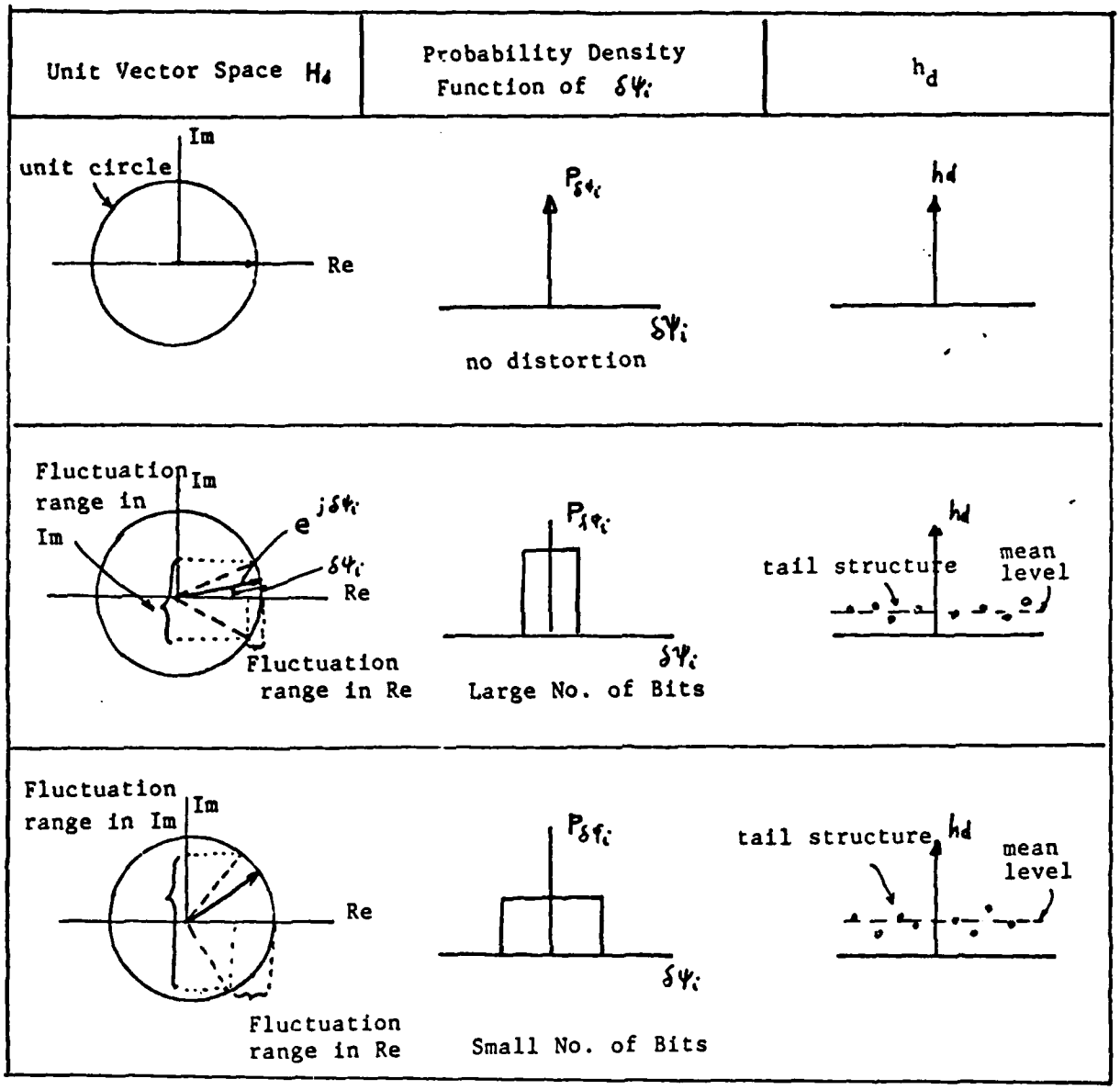

Figure 8. Illustration of Analysis of h_d for Phase Distortion

the product of the lower bound correlation coefficient ρ_0 and the transfer index K.

ρ_0 can be further decomposed into two independent factor: ρ_A, the amplitude correlation coefficient, and ρ_{Σ}, the phase-dependent correlation factor. For optimum quantization, the amplitude correlation coefficient ρ_A is equal to the rms value of the quantizer output level a_i' normalized to the rms value of the input data, with the input ranges chosen such that the optimum conditions of (2.6a) and (2.6b) are met. For the case of the phase being uniformly distributed, the phase-dependent correlation factor ρ_{Σ} is the sinc function of π / N_{Σ} where N_{Σ} is the number of output levels. For Rayleigh distributed amplitude and uniform distributed phase, ρ_0 is independent with the statistical properties (mean or variance) of the image data and uniquely related to the entropies of the quantized signals.

The transfer index K is completely specified when the distributions of the aperture data and the quantizer parameters are given. Given number of quantized levels, K is insensitive to the changes in the setting of output levels. It has also shown that K is asymptotically independent with amplitude distribution and insensitive to the variations of the phase distribution. Therefore, K is nearly a scene-free parameter.

2) The optimum quantization scheme, which maximizes $\rho_0$for a given number of output levels, consists of two independent quantizers, an amplitude quantizer and a phase quantizer. For each quantizer, the output level from each quantizer-established-range is equal to the conditional mean of the input over that range. The value of the dividing point (endpoint) between any two quantizer-established-ranges is equal to the arithmetic mean of the conditional means of the two adjacent ranges. These are the two conditions for optimum quantization {(2.6a)-(2.6d)}. This optimum scheme is good for an arbitrary amplitude distribution and for a uniform phase distribution.

3) The theory of Bit Compression for microwave imaging is developed by presenting an exact solution of the analytic equation of image correlation coefficient in terms of the entropy of the

quantized aperture data through the optimum quantization procedure. For a given distribution of complex aperture data, the theory determines the minimum number of bits required of the quantized signal for the image to achieve any given quality or, conversely, what quality of image can be obtained for any given number of bits that the quantized signal retains. It proves that the phase information thoroughly dominates the process. It is shown that hard limiting the input to a phased array while leaving the phase unaltered preserves much of the image integrity. Amplitude-only information destroys it. Hard limiting plus one bit of phase information sometimes suffices. Hard limiting plus two bits of signal phase per sample often results in acceptable imagery. A minimum of 4 bits of information per complex signal sample guarantees a relatively good image provided that 3 bits are used to represent the phase and 1 bit is used to represent the amplitude. Eight bits are required to ensure a high fidelity image.

4) The theory provides a rule of thumb for optimum bit allocation between amplitude quantizer and phase quantizer. It indicates that when the number of bits per data sample is no more than 8, the number of bits assigned to phase should be two larger than the number of bits assigned to amplitude. For finer quantization, equal numbers of bits should be assigned to amplitude and phase.

5) The theory imposes substantially no constraints upon the distributions of amplitude and phase in the microwave data. It is also shown that the optimum quantization design derived from the theory is nearly scene-independent and may achieve real-time performance.

6)Finally, the theory provides guidelines to explore the nature of distortion due to data compression. It is shown that the distorted energy is spread all over the image plane. Its major effect is to increase the noise level so that the dynamic range will be decreased.

REFERENCES

[1] A. K. Jain, "Image Data Compression: A Review," IEEE Proc., vol. 69, No. 3, pp. 349-389, March 1981.

[2] B. D. Steinberg, "Microwave Imaging with Large Antenna Arrays, Radio Camera Principles and Techniques," New York: John Wiley & Sons, Inc., 1983.

[3] J. D. Kraus, 3rd ed. "Eletromagnetics," New York: McGraw-Hill Inc.,1984.

[4] B. D. Steinberg, "Principles of Aperture and Array System Design: Including Random and Adaptive Arrays," New York: John Wiley and Sons, Inc., 1976.

[5] B. D. Steinberg, "A Theory of The Effect of Hard Limiting and Other Distortions Upon The Quality of Microwave Images," IEEE Trans. Acoust. Speech Signal Processing, vol. 35, No. 10, pp. 1462-1472, Oct. 1987.

[6] S. M. Kay and J. H. Marple, "Spectrum Analysis - A Modern Perspective," Proc. IEEE, vol.69, No. 11, pp. 1380-1419, Nov.1981.

[7] A. Papoulis, 2nd ed. "Probability, Random Variables, and Stochastic Processes," New York: McGraw-Hill Inc., 1984.

[8] K. Max "Quantizing for Minimum Distortion," IRE Trans. Inform. Theory, vol. 6, pp. 7-12, March 1960.

[9] M. D. Paez and T. H. Glisson, "Minimum Mean Squared-Error Quantization in Speech," IEEE Trans. Comm., vol. 20, pp. 225-230, April 1972.

[10] Neal C. Gallagher, Jr. "Quantizing Schemes for The Discrete Fourier Transform of A Random Time Series," IEEE Trans. Inform. Theory vol. 24, No. 2, March 1978.

[11] J. D. Bruce, "Optimum Quantization," Research Lab of Electronics, MIT, Cambridge, Tech. Rept. 429, March 1965.

[12] Dhiraj K. Sharma, "Design of Absolutely Optimal Quantizers for A Wide Class of Distortion Measures," IEEE Trans. Inform. Theory, vol. 24, No. 6, pp. 693-702, Nov. 1978.

[13] E. D. Banta, "Far Field Properties of Wide Band Planar Arrays with Nonlinear Processing," IRE Convention Record, Part I, pp. 95-100, 1961.

[14] J. J. Kovaly and S. N. Miller, "A Superlimiting Phased-Array Receiving System in a Two-Source Environment," IEEE Trans. Aerosp. Electron. Syst., vol. 3, pp. 518-526, May 1967.

[15] D. Kermish, "Image Reconstruction from Phase Information Only", J. Opt. Soc. Am., vol 60, No.1, pp. 15-16, Jan. 1970.

[16] P.L. Van Hove, J. S. Lim, A. V. Oppenheim, "Signal Reconstruction from Fourier Transform Amplitude," Technical Digest, Topical Meeting on Signal Recovery and Synthesis with Incomplete Information and Partial Constraints, Nevada, pp. 12-14, Jan. 1983.

[17] P. L. Van Hove, M. H. Hayes, J. S. Lim, and A. V. Oppenheim, "Signal Reconstruction from Signed Fourier Transform Magnitude," IEEE Trans. Acoust. Speech Signal Processing, vol. 31, No. 5,pp. 1286-1293, Oct. 1983.